

GT2014-26014

AN ACCELERATED MEDIAL OBJECT TRANSFORMATION FOR WHOLE ENGINE OPTIMISATION

Leran Wang, David J. J. Toal and Andy J. Keane
University of Southampton
Southampton, UK
Email: lw2c09@soton.ac.uk

Felix Stanley
Rolls-Royce plc.
Derby, UK
Email: Felix.Stanley@Rolls-Royce.com

ABSTRACT

The following paper proposes an accelerated medial object transformation for the tip clearance optimisation of whole engine assemblies. A considerable reduction in medial object generation time has been achieved through two different mechanisms. Faces leading to unnecessary branches in the medial mesh are removed from the model and parallelisation of the medial object generation is improved through the subdivision of the original 3D CAD model. The time savings offered by these schemes are presented with respect to the generation of the medial objects of two complex gas turbine engine components. It is also demonstrated that the utilization of these techniques within a design optimisation may result in a considerable reduction in wall time.

INTRODUCTION

During the preliminary design stage, engineers often want to investigate as many different designs as possible before proceeding to the detailed stage. However, due to the large number of design variables in a complete engine and the time-consuming nature of 3D finite element simulations, the optimisation of one design may take weeks or even months to perform. A 3D finite element mesh typically contains several million degrees-of-freedom (DOF) and one single simulation may take hours or perhaps days to complete [1]. Previous whole engine optimisations, such as those of Toal et al. [2], for example, employed whole engine transient thermo-mechanical simulations taking several days to evaluate even on a high performance compute cluster and resulted in design optimisations taking months to perform. Due to this time restriction the number of variables included in a de-

sign optimisation tends to be very small which may potentially lead to a suboptimal design.

Vouchkov et al. [3] took a slightly different approach to whole engine design optimisation by developing a simplified shell and beam model of the engine and employing this within a multi-objective evolutionary based design search. The low cost of the engine simulations made such an optimisation possible but the considerable effort in the manual construction of such shell and beam models still makes such an optimisation prohibitively expensive. The model also has no direct link to the 3D geometry making it difficult to transfer the optimal shell thicknesses back into a usable CAD model.

A whole engine design optimisation scheme is therefore required which has the speed of a shell and beam based model but which can be directly linked to 3D CAD and is able to represent all of the complex features of such a CAD model.

In order to increase the speed of finite element analyses (FEA), dimensional reduction and mixed dimensional modelling techniques have attracted considerable interest. Thakur et.al [4] published a review paper on current model simplification techniques for a variety of purposes among which medial object transformation was identified as being an extremely useful dimensional reduction tool for FEA idealization.

Most existing medial object transformation techniques are based on the medial axis transform (MAT) [5]. The MAT represents the medial line (in 2D) or the medial surface (in 3D) of a given 2D surface or 3D solid. Imagine a maximal inscribed disc rolling along a surface or a maximal inscribed ball rolling around a solid, the medial trace and the radius at each medial point forms the MAT [6] (Fig.1(a)). The MAT is a complete and unique rep-

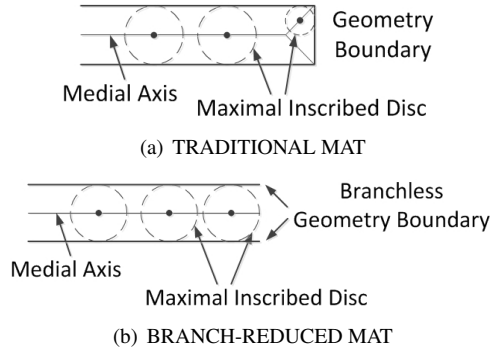


FIGURE 1. COMPARISON OF TWO MATS

representation of the original shape and one can regenerate the exact original shape based on the MAT. Once an optimisation has been performed using the MAT this relationship can potentially allow the corresponding solid geometry to be generated.

Rather than perform a complete transformation from the original CAD geometry into a medial object, alternative approaches have also been explored within the literature to create models of mixed dimensions with the view to the FEA simulations being more accurate than a simulation employing a pure medial object.

The mixed dimensional modelling technique, for example, creates a mixed dimensional idealization from the CAD geometry. Firstly the geometry is classified into one of three types, thin-sheet, long-slender and complex regions. The identified thin-sheet regions are meshed with shell elements, the long-slender regions with beam elements and the complex regions with tetrahedral elements [7–10].

Other similar work within the literature includes the mid-surface generation for non-manifold geometry [11] and the MAT based on identifying face pairs [12, 13].

Unlike most existing MAT techniques which require a solid geometry as an input, the medial mesh generation process employed in this work only requires a surface triangulation [14] and calculates the medial mesh based on a surface mesh of the 3D geometry. Whilst the medial mesh resulting from this process can be directly used for structural analysis, the unique methodology employed in its generation allows faces of the original geometry to be ignored from the process thereby removing unnecessary branches from the final model and the original geometry to be easily subdivided to greatly improve parallelisation of the medial object generation. Fig.1(b) demonstrates the MAT based on a branch-reduced geometry boundary.

Although not considered within the presented work it should also be recognised that the generated medial mesh can also be used to help construct a high-quality volume mesh [15, 16] for further analysis or as part of a multi-fidelity design optimisation [17–19].

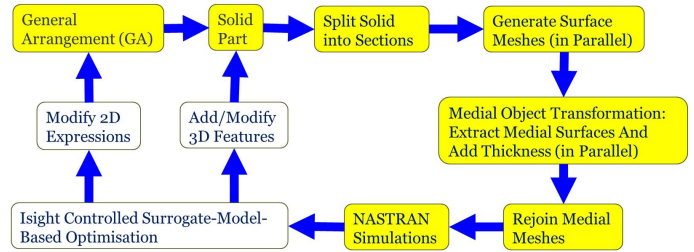


FIGURE 2. PROPOSED WHOLE ENGINE OPTIMISATION WORK FLOW

The accelerated medial object transformation presented in this paper is a key component within a proposed whole engine optimisation work flow. The main objective of the optimisation work flow is to perform tip clearance studies at the preliminary design stage. Therefore only casing displacement results are presented in the following sections. However, once a set of designs have been chosen from the optimisation Pareto front, further detailed structural analyses could be performed. As shown in Fig. 2, the process commences by creating a datum engine model by revolving a fully-parameterised gas turbine general arrangement (GA) to which 3D components are applied from a library of user defined features (UDFs). Instead of a traditional 3D finite element simulation, a 3D medial surface mesh (2D shells) is then extracted from the 3D geometry. As will be illustrated in the following paper, this process is accelerated by ignoring unnecessary medial branches and splitting the solid geometry into several sections. The medial mesh extraction for each section is then performed in parallel with the separate meshes then combined to form the complete medial mesh which can be simulated using NASTRAN. As will be demonstrated, carrying out such simulations using this mesh offers a considerable reduction in simulation cost with little loss in accuracy.

Although not presented within the current paper, it is proposed that the medial mesh simulations are then post-processed and the calculated objective function values employed within a surrogate model based optimisation [20]. Those boxes of Fig. 2 highlighted in yellow represent the work presented within the current paper.

The following paper commences with a short discussion of the creation of the test case geometry used throughout the remainder of the paper. This is followed by a description of processes by which the proprietary Rolls-Royce medial mesh generation software can be accelerated. The paper then concludes by presenting the performance of the medial object generation process and any resulting FEA simulations with respect to two gas turbine engine casings.

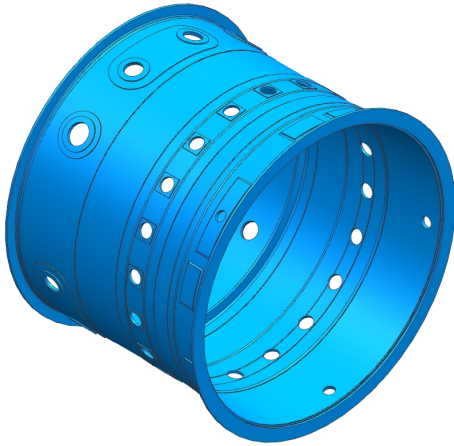


FIGURE 3. COMBUSTION CHAMBER OUTER CASING CAD MODEL

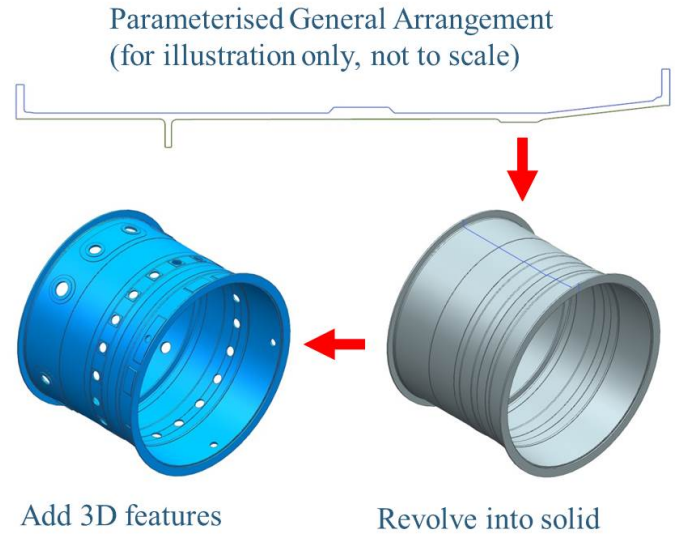


FIGURE 5. GEOMETRY GENERATION OF A CCOC

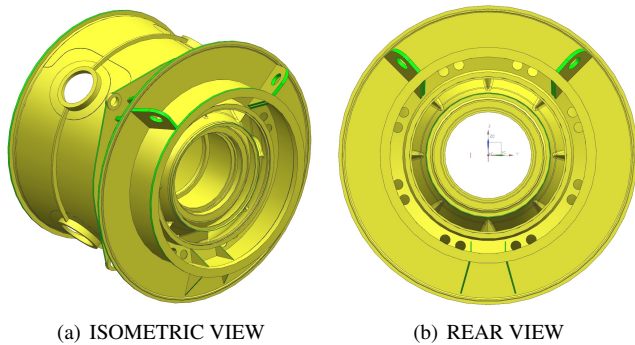


FIGURE 4. COMPRESSOR INTERCASING CAD MODEL

GAS TURBINE TEST CASE GEOMETRIES

The presented work aims to demonstrate the efficiency of the medial axis generation part of the proposed design optimisation work flow highlighted in Fig. 2. To do so two gas turbine engine casings will be used, a combustion chamber outer casing (CCOC), Fig. 3 and a compressor inter casing, Fig. 4.

Both the CCOC and inter casing geometries are generated in a similar manner. The portion of the engine general arrangement (GA) relating to each section is first parameterised using Siemens NX. Although not illustrated within the current paper, this parameterisation permits the modification of important features such as casing thicknesses and flange heights in any future design optimisation. The parameterised GA is then revolved to form a solid model to which parametric 3D features are then added. The parameters defining the shape of these 3D features could also be altered within any future optimisation. Figure 5 demonstrates the geometry generation process using the CCOC model as an example. A similar process was also used to create the inter casing model but, as can be clearly seen, this required

the addition of many more 3D features.

While both the CCOC and inter casing models illustrated in Figures 3 and 4 are somewhat simplified from what would be expected at the detailed design stage, they are still representative of the complexity of an actual gas turbine engine. Features which are important for the structural analysis, such as bosses, holes and struts are included in order to create casing models which behave realistically under load.

ACCELERATED MEDIAL MESH GENERATION

Throughout this paper all medial meshes are extracted using the proprietary, Rolls-Royce, medial mesh generation software, MANTLE (Modelling and Analysis in the Neutral Line). Full details of the methodology followed by MANTLE in the creation of a medial mesh can be found in the thesis of Stanley [14]¹. The presented work demonstrates how the preparation of the surface mesh of the original geometry can accelerate the MANTLE medial mesh extraction process.

Before presenting the methodologies for accelerating the process let us first consider the medial axis generation itself. Fig.6 uses a 1/12 axisymmetric section of the CCOC to demonstrate the medial mesh extraction process. The inputs to MANTLE are the 2D surface meshes (8,152 CTRIA3 elements and each node has 6 DOFs) of the solid part (Fig.6(a)). Because MANTLE has the capability to automatically refine the element sizes around geometry changes, a coarse surface mesh is sufficient to generate a good quality medial mesh. In this particular case an initial element size of 10mm has been used, Fig.6(b)

¹Medial mesh generation, patent number GB1300259.7

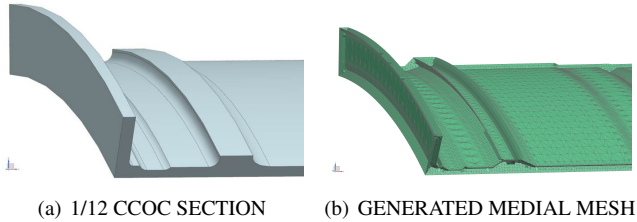


FIGURE 6. AN EXAMPLE MEDIAL MESH GENERATION

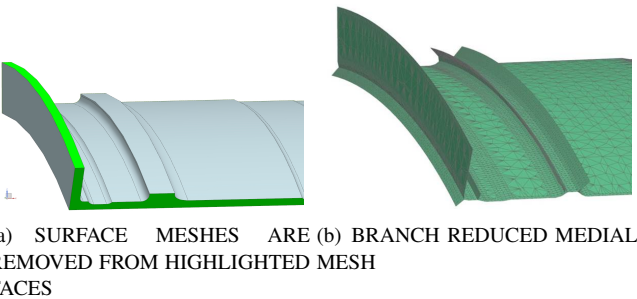


FIGURE 7. GENERATION OF BRANCH REDUCED MEDIAL MESH

illustrates the resulting medial mesh which consists of 51,529 CTRIA3 shell elements with each element having an independent thickness value assigned.

In Fig.6(b) it can clearly be observed that the medial mesh contains branches at the top of the flange and at the side of the section. These branches are generally undesirable because it takes MANTLE a long time to compute the nodes along them and they add extra mass to the geometry. Unlike most existing medial surface generation tools which require solid geometry as an input, as MANTLE calculates the medial mesh using surface meshes it is possible to reduce the branches in the medial mesh by removing the corresponding surface meshes from the input (Fig.1(b)). As shown in Fig. 7, if the surface meshes are removed from the highlighted faces in Fig. 7(a), the generated medial mesh will be branch reduced (Fig. 7(b)). The branch-reduced input surface mesh and the generated medial mesh have 7,304 and 41,130 CTRIA3 elements respectively, both of which contain less elements than the model with branches. As a result, the medial mesh generation time has been reduced by 30% in this particular case.

The ability of MANTLE to create such branchless medial models also permits the entire process to be easily parallelised. Generally the simpler the geometry model the quicker a medial mesh can be generated. In theory it therefore makes sense to subdivide a large CAD model into a number of smaller sub-models with the medial mesh for each calculated in parallel. This process proves to be complicated using traditional algorithms because they have no knowledge of where the splits in the geometry are

and would treat the defining faces of such splits as they would any other face in the geometry and create branches.

Figure 6(b) also helps to illustrate this. Here an axisymmetric CAD model has been split into 12 identical sub-sections. But when the medial axis is generated branches are included along the split faces. Copying this medial mesh around the axis of the engine twelve times and combining them into a single mesh would result in ridges along the casing and an incorrect FEA solution.

MANTLE's branchless capability permits the surface mesh defining such splits to be left out of the medial mesh generation process producing the mesh in Fig. 7(b) which can be easily copied around the engine's axis to produce a correct medial mesh.

Using the same process it is therefore possible to split the original geometry into a series of sub-models and take full advantage of any inherent symmetry within the model. This reduces the overall medial mesh generation time as a number of smaller sections can be run in parallel and also, by taking advantage of any inherent symmetry, fewer medial meshes may be required. Medial mesh extraction time is therefore dependant on the largest sub-section plus the time used for combining them. The identification of branchless surfaces and the splitting of the geometry requires negligible manual effort comparing to the optimisation work flow as the two processes only need to be carried out once. In Siemens NX this is done by tagging the appropriate faces to be ignored and splitting the solid. It is preferable to split the solid along simple planes rather than to cut through complex geometries because the medial mesh is automatically refined around the split regions and a simpler plane cut will introduce fewer additional shell elements. It is also possible to automate both processes using user defined functions (UDFs). As shown in Fig.1(b) and 7, the branchless medial mesh still reaches the very end of geometry boundaries, therefore there will be no gaps between adjacent sections. The nodes on the adjacent medial mesh edges are aligned automatically by MANTLE which is easy to achieve because the input surface meshes all have matching nodes along the edges.

CASE STUDY 1: CCOC

Having described the proposed methods of accelerating medial mesh generation using MANTLE let us now consider the impact of these methods on the two gas turbine casing geometries described previously. Consider first the CCOC casing presented in Fig. 3.

Creating a medial mesh of the CCOC geometry in a single operation and including all faces will take a considerable amount of time, approximately 64 times that taken to generate a 3D tetrahedral mesh (TETRA10 element where each node has 3 DOFs) using Siemens NX. However, by reducing the number of branches in the medial mesh by removing the faces on the tops

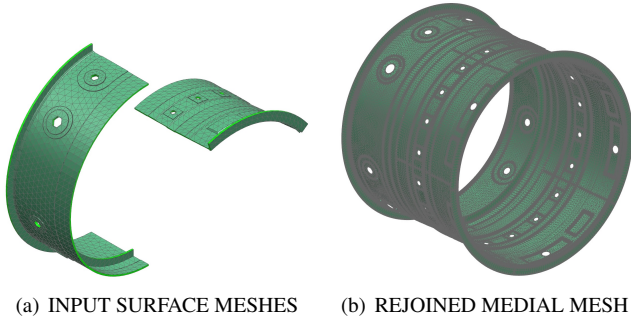


FIGURE 8. CCOC MEDIAL MESH GENERATION BY SPLITTING AND REJOINING

TABLE 1. COMPARISON OF MESHING AND SIMULATION TIMES FOR DIFFERENT CCOC MEDIAL MESH GENERATION SCHEMES

| | Full | Branch Reduced | Split |
|-------------------------------|--------------|----------------|--------------|
| Relative Mesh Generation Time | $\times 64$ | $\times 53$ | $\times 18$ |
| Relative FE Simulation Time | $\times 0.7$ | $\times 0.7$ | $\times 0.7$ |

of the flanges and inside the holes illustrated in Fig. 3 reduces the cost of the medial mesh generation by approximately 17% to 53 times the cost of creating a 3D tetrahedral mesh.

Let us now consider the impact of parallelising the generation of the same medial mesh. Figure 8 demonstrates the parallelisation process implemented on the CCOC. In this case the geometry is split into 7 sections. The two front sections are symmetric and the five rear sections are axisymmetric. Therefore it is only necessary to generate the medial meshes for two sections, as shown in Fig.8(a). As required each mesh is mirrored or rotated and combined to create a complete mesh, (Fig.8(b)). Figure 8(b) also illustrates MANTLE’s automated refinement process, the additional elements along the splits can be clearly seen. Using this parallelised approach the medial mesh extraction time has been further reduced to 18 times that of the 3D tetrahedral mesh a 66% increase in efficiency over the baseline approach of calculating the complete mesh at once. It should also be noted that this 66% improvement includes the same branch reduction previously applied. Table 1 presents a summary of the times taken to create the medial mesh for the CCOC relative to create a 3D tetrahedral mesh.

It is also worth noting that the efficiency increase in wall time does not depend on the whether the geometry has symmetric or axisymmetric properties. As multi-core computers are commonplace nowadays, the surface mesh can be split into multiple sections and fed into MANTLE in parallel. Exploring symmetric and axis-symmetric properties will, however, save total computational cost.

With a branchless medial mesh of the CCOC obtained let

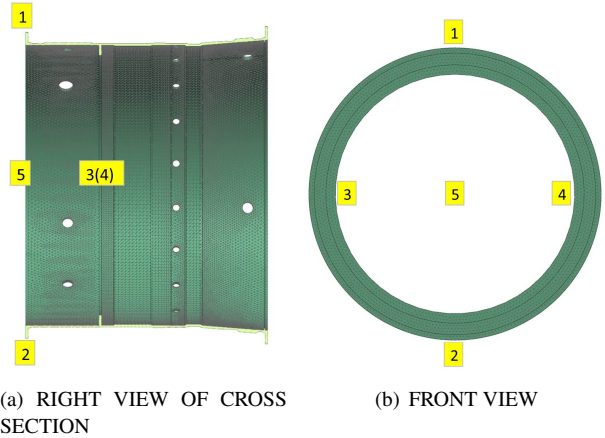


FIGURE 9. LOCATION OF POINTS AROUND CCOC AT WHERE THE DISPLACEMENTS WERE MEASURED

us now consider how it impacts on the speed and accuracy of any FE simulation. The medial mesh illustrated in Fig. 8(b) is therefore compared directly to a 3D FE simulation employing the unstructured tetrahedral mesh used to define the relative costs of the medial mesh generation.

Simulations involving a total of five load cases were set up and carried out using the 3D and medial mesh. In each case, the CCOC is constrained at the rear. Four loads, namely axial, radial, yaw and torque, were applied to the front of the casing while the fifth load case involves a simulation of gravity. The results show that a simulation using the medial mesh takes 70% of the time required to run a 3D simulation. As the medial mesh is almost identical in all cases, the time savings over the 3D simulation are identical in Tab. 1.

The displacements for both the full 3D tetrahedral mesh and the generated medial mesh were measured at five different locations around the CCOC casing, illustrated in Fig.9. Location five corresponds to the master node through which the forces for the first four load cases are applied. The percentage differences between the 3D simulation and the medial mesh results at each of these locations and their maximum and root-mean-square (RMS) values are listed in Tab. 2 for each load case.

Overall there is very little difference in the displacements between the two simulations. Of the five load cases the difference in the displacements at the majority of locations was below 6%, well within acceptable bounds. Only the radial load case appeared to produce errors above this value, but even then the medial simulation was still only 8.26% from the 3D simulation.

As explained during the introduction, during an optimisation process the medial mesh only needs to be generated once if changes are made to only the thickness values defining the mesh. In such a case updates to the medial mesh are almost instantaneous. The 3D FE simulation, however, requires a new mesh to be generated after every geometry manipulation. This continual

TABLE 2. PERCENTAGE DIFFERENCE OF SIMULATION RESULTS BETWEEN 3D AND MEDIAL MESHES (CCOC)

| Load type | Axial | Radial | Yaw | Torque | Gravity |
|-------------|-------|--------|-------|--------|---------|
| Max % diff | 7.29 | 8.26 | 4.04 | 5.93 | 5.85 |
| RMS % diff | 5.67 | 7.02 | 2.65 | 3.86 | 4.56 |
| % diff at 1 | 6.60 | -7.06 | -1.51 | 1.60 | -2.62 |
| % diff at 2 | 7.29 | -7.40 | -1.61 | 1.96 | -5.53 |
| % diff at 3 | -5.44 | -6.04 | -4.04 | -5.93 | -3.63 |
| % diff at 4 | -5.15 | -6.10 | -3.43 | -5.53 | -5.85 |
| % diff at 5 | -2.84 | -8.26 | -1.44 | -1.53 | -4.38 |

TABLE 3. COMPARISON OF MESHING AND SIMULATION TIMES FOR DIFFERENT INTERCASING MEDIAL MESH GENERATION SCHEMES

| | Full | Branch Reduced | Split |
|-------------------------------|-------|----------------|-------|
| Relative Mesh Generation Time | ×515 | ×468 | ×99 |
| Relative FE Simulation Time | ×0.33 | ×0.33 | ×0.33 |

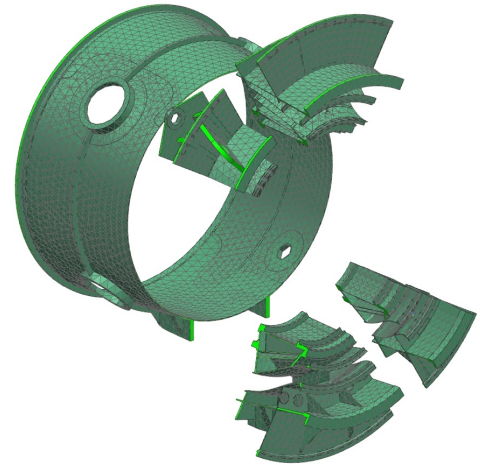
meshing, coupled with the increased cost of the FE simulation, means that even with the initially high cost of the medial mesh generation taken into account the medial approach will eventually be more efficient than the full 3D approach.

In the case of the generating the medial mesh in a single pass without branch reduction this point occurs after 50 iterations, a number which could be easily surpassed within an optimisation process. Reducing the number of branches reduces this to approximately 41 iterations whereas employing an efficient parallelisation reduces this to approximately 14 iterations. A number easily surpassed when performing a relatively small design of experiments.

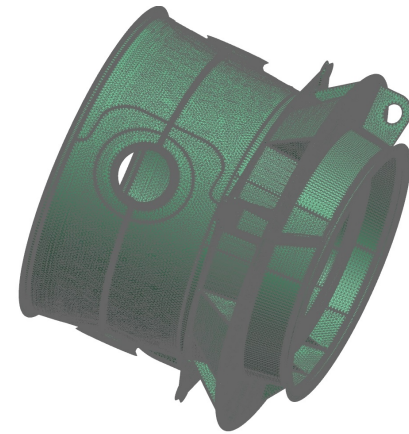
CASE STUDY 2: COMPRESSOR INTERCASING

The previous section illustrated the advantages of medial mesh generation using the CCOC as an example. Since the CCOC is a relatively simple geometry let us now apply the same techniques to the more complex compressor intercasings illustrated in Fig.4.

The highlighted faces in Fig.4 indicate where the surface meshes are not evaluated in order to generate a branch reduced medial mesh. This has the effect of reducing the cost of the medial mesh generation by approximately 9% from 515 times the cost of the 3D tetrahedral mesh to 468 times. It should be noted at this point that Tab. 3 presents the cost of creating the medial mesh using the three different approaches relative to that of cre-



(a) INPUT SURFACE MESHES



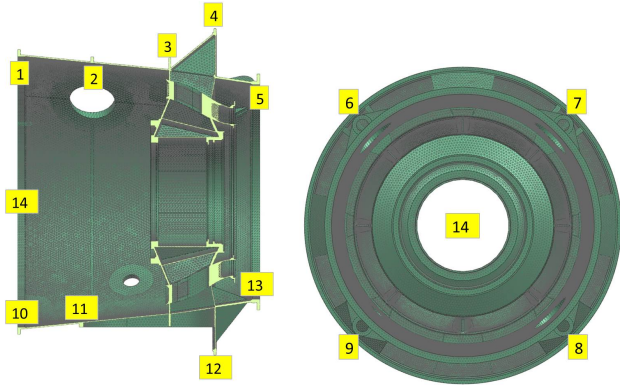
(b) REJOINED MEDIAL MESH

FIGURE 10. INTERCASING MEDIAL MESH GENERATION BY SPLITTING AND REJOINING

ating a 3D tetrahedral mesh using Siemens NX. Also presented in Tab. 3 is the cost of performing the FE simulation using the medial mesh relative to performing a FE simulation using the 3D mesh.

As with the CCOC, the inter casing can be split into 9 sections, one front cylinder and 8 rear fan-shaped sections. Taking the symmetric and axis-symmetric properties into consideration, it is only necessary to generate the medial meshes for 5 sections, as shown in Fig.10(a). Employing this approach the medial mesh generation time is reduced to 19% of the baseline medial mesh generation approach which is equivalent to 99 times the cost of generating a 3D mesh. The final medial mesh is illustrated in Fig.10(b).

Now that we have a medial mesh let us consider its application within a FE simulation. In a similar manner to the CCOC both the medial and 3D meshes have been used to simulate five



(a) RIGHT VIEW OF CROSS SECTION

(b) FRONT VIEW

FIGURE 11. LOCATION OF POINTS AROUND INTERCASING WHERE DISPLACEMENTS ARE MEASURED

load cases. In each case, the inter casing is constrained at the rear with axial, radial, yaw and torque loads applied at the front of the casing. As with the CCOC the fifth load case considers the action of gravity. As per the CCOC above a global mesh size of 5mm was used to construct the 3D mesh. In this case a simulation of the inter casing using the medial mesh is approximately 33% of the cost of a fully 3D simulation. Even with the initial expense of the medial mesh generation this large reduction in simulation time means that an optimisation employing the medial approach only requires 20 iterations to become more efficient than the 3D FE approach.

Given the reduction in relative simulation cost compared to the full 3D simulation as the complexity of the 3D geometry increased from the CCOC to the inter casing, one would expect a medial mesh based simulation of an entire engine to be extremely efficient. Likewise given the modular design of a modern gas turbine engine and the presence of multiple symmetric features one would expect the medial mesh generation to be very parallelisable. The presented technology therefore has the potential to offer huge performance gains when applied to a whole engine assembly.

The results of these simulations are compared at 14 different locations around the inter casing, illustrated in Fig.11. The percentage differences at these points between the two simulations and the maximum and RMS values are listed in Table 4.

As with the CCOC the results of the medial mesh simulation are quite close to those of the 3D simulation. In the worst case the medial mesh simulation is 10.36% away from the 3D simulation but, on average for each load case, the simulations are within less than 8%.

TABLE 4. PERCENTAGE DIFFERENCE OF SIMULATION RESULTS BETWEEN 3D AND MEDIAL MESHES (INTERCASING)

| Load type | Axial | Radial | Yaw | Torque | Gravity |
|--------------|--------|--------|-------|--------|---------|
| Max % diff | 10.34 | 7.29 | 7.61 | 9.20 | 10.36 |
| RMS % diff | 6.69 | 4.91 | 5.00 | 7.83 | 7.44 |
| % diff at 1 | 7.54 | -5.61 | -4.10 | -5.35 | -9.37 |
| % diff at 2 | -3.20 | -5.04 | -4.84 | -6.67 | -9.11 |
| % diff at 3 | -5.99 | -5.97 | -4.65 | -9.16 | -8.45 |
| % diff at 4 | -6.04 | -5.42 | 3.53 | -9.17 | -7.90 |
| % diff at 5 | -6.08 | -3.13 | -5.55 | -7.79 | -5.53 |
| % diff at 6 | -7.95 | -5.45 | -5.87 | -8.70 | -8.27 |
| % diff at 7 | -7.30 | -4.95 | -5.99 | -8.70 | -4.66 |
| % diff at 8 | -10.23 | -7.11 | -5.83 | -9.12 | 2.20 |
| % diff at 9 | -10.34 | -7.29 | -6.28 | -9.05 | 10.36 |
| % diff at 10 | 1.97 | -2.61 | -1.56 | -4.52 | -5.20 |
| % diff at 11 | -3.25 | -1.78 | -1.65 | -5.44 | -5.21 |
| % diff at 12 | 1.07 | 0.00 | 3.13 | -9.20 | -7.81 |
| % diff at 13 | -3.57 | -1.18 | -5.35 | -8.24 | -9.21 |
| % diff at 14 | -9.69 | -6.04 | -7.61 | 6.13 | -6.20 |

CONCLUSIONS

This paper presents the authors' efforts to reduce the cost of medial object generation through branch removal and parallelisation as part of the development of an efficient whole engine design optimisation framework. Employing these approaches it has been demonstrated that a medial mesh based simulation is faster than a traditional 3D simulation with comparable accuracy. For an optimisation of more than 20 iterations employing a medial mesh based process will be more efficient than 3D simulations, even with the overhead of generating the medial mesh. Given the potential number of design variables in a simple component like a CCOC, an optimisation would easily exceed this number of iterations. An optimisation of the presented inter casing geometry, employing 100 iterations would be completed in less than half the time of the equivalent optimisation employing 3D simulations. This efficiency gain is expected to continue to grow further if larger whole engine assemblies were to be considered in the future.

Whilst the presented work has focused on geometry preparation and medial mesh generation, future work will embed it within a surrogate model based optimisation.

ACKNOWLEDGMENT

The research leading to these results has received funding from the European Community's Seventh Framework Programme (FP7/2007-2013) under grant agreement NO. 314366. The authors also acknowledge Rolls-Royce for granting permission to publish this paper.

REFERENCES

- [1] Benito, D., Dixon, J., and Metherell, P., June 9-13, 2008. "3D thermo-mechanical modelling method to predict compressor local tip running clearances". In Proceedings of ASME Turbo Expo 2008: Power for Land, Sea, and Air, pp. 1589–1598.
- [2] Toal, D., Keane, A., Benito, D., Dixon, J., Yang, J., Price, M., Robinson, T., Remouchamps, A., and Kill, N., 2013. "Multi-fidelity multidisciplinary whole engine thermo-mechanical design optimization". *Journal of Propulsion and Power*, (**Under Review**).
- [3] Voutchkov, I., Keane, A., and Fox, R., 2006. "Robust structural design of a simplified jet engine using multiobjective optimization". In 11th AIAA/ISSMO Multidisciplinary Analysis and Optimization Conference.
- [4] Thakur, A., Banerjee, A., and Gupta, S., 2009. "A survey of cad model simplification techniques for physics-based simulation applications". *Computer-Aided Design*, **41**(2), p. 6580.
- [5] Blum, H., 1967. *A transformation for extracting new descriptors of shape*. MIT Press, Cambridge, MA, pp. 362–380.
- [6] Robinson, T., Armstrong, C., Lee, K.-Y., and Ou, H., 6-8 June, 2006. "Automated mixed dimensional modelling for the finite element analysis of swept and revolved cad features". In Proceedings of the 2006 ACM symposium on Solid and physical modelling, p. 117128.
- [7] Robinson, T., Armstrong, C., Lee, K.-Y., and Ou, H., 21-22 March, 2005. "Automatic mixed dimensional finite element modelling of sketch based cad components". In 13th ACME CONFERENCE.
- [8] Robinson, T., Fairey, R., Armstrong, C., Ou, H., and Butlin, G., October 1215, 2008. "Automated mixed dimensional modelling with the medial object". In Proceedings of the 17th International Meshing Roundtable, pp. 281–298.
- [9] Robinson, T., Armstrong, C., and Fairey, R., 2011. "Automated mixed dimensional modelling from 2D and 3D CAD models". *Finite Elements in Analysis and Design*, **47**(2), p. 151165.
- [10] Nolan, D., Tierney, C., Armstrong, C., Robinson, T., and Makem, J., 2013. "Automatic dimensional reduction and meshing of stiffened thin-wall structures". *Engineering With Computers*.
- [11] Chong, C., Kumarb, A., and Lee, K., 2004. "Automatic solid decomposition and reduction for non-manifold geometric model generation". *Computer-Aided Design*, **36**(13), p. 13571369.
- [12] Ramanathan, M., and Gurumoorthy, B., 2003. "Constructing medial axis transform of planar domains with curved boundaries". *Computer-Aided Design*, **35**(7), p. 619632.
- [13] Yin, L., Luo, X., and Shephard, M., September 11-14, 2005. "Identifying and meshing thin sections of 3-d curved domains". In Proceedings of the 14th International Meshing Roundtable, pp. 33–54.
- [14] Stanley, F., 2010. "Dimensional reduction and design optimization of gas turbine engine casings for tip clearance studies". Doctoral Thesis, University of Southampton, Southampton, UK.
- [15] Sampl, P., 2001. "Medial axis construction in three dimensions and its application to mesh generation". *Engineering With Computers*, **17**(3), pp. 234–248.
- [16] Makem, J., Armstrong, C., and Robinson, T., 2012. "Automatic decomposition and efficient semi-structured meshing of complex solids". *Engineering with Computers*.
- [17] Forrester, A., Sobester, A., and Keane, A., 2007. "Multi-fidelity optimization via surrogate modelling". *Proceedings of the Royal Society A*, **463**(2088), pp. 3251–3269.
- [18] Brooks, C., Forrester, A., Keane, A., and Shahpar, S., 2011. "Multi-fidelity design optimisation of a transonic compressor rotor". In 9th European Turbomachinery Conference, Istanbul, Turkey, 21st-25th March.
- [19] Toal, D., and Keane, A., 2011. "Efficient multi-point aerodynamic design optimization via co-kriging". *Journal of Aircraft*, **48**(5), pp. 1685–1695.
- [20] Forrester, A., Sobester, A., and Keane, A., 2008. *Engineering Design via Surrogate Modelling: A Practical Guide*. John Wiley & Sons, Ltd, Chichester, UK.